Available online at www.sciencedirect.com

SCIENCE DIRECT®

Catalysis Today 102–103 (2005) 115–120

CATALYSIS TODAY

www.elsevier.com/locate/cattod

Catalytic filamentous carbons-supported Ni for low-temperature methane decomposition

T.V. Reshetenko [*], L.B. Avdeeva, Z.R. Ismagilov, A.L. Chuvilin, V.B. Fenelonov

Boreskov Institute of Catalysis, Pr. Akad. Lavrentieva 5, Novosibirsk 630090, Russia

Abstract

Ni/CFC catalysts were shown to have sufficient efficiency in secondary carbon formation in low-temperature methane decomposition (525 °C). The highest yield of secondary carbon was found to reach 268.5 g/g_{Ni} on Ni/CFC (Fe–Ni) catalyst. The catalytic properties of Ni/CFCs may be explained by formation of active Ni particles (ca. 50 nm in size), which are optimal for growth of filament with "herring-bone" structure. The large Ni particles are preferably localized in the pores formed by interlaced filaments and the interaction of metal particles with graphene basal planes occurs mainly through weak dispersive forces. The accumulation of carbon on Ni/CFC catalysts is also influenced by textural properties of the used supports. The carbon supports with high value of the meso- and macropore volume are likely to be more suitable for development of Ni/CFC catalysts for low-temperature methane decomposition. The modification of the textural properties of catalytic filamentous carbon (CFC) by their activation with H_2 or CO_2 opens up interesting possibilities of its application as support in heterogeneous catalysis.

Keywords: Carbon filaments; Carbon nanotubes; Gasification; Texture; Catalyst support

1. Introduction

The last decade showed an increasing fundamental and practical interest in carbon nanotubes and nanofibers. The family of catalytic filamentous carbon (CFC) is novel turbostratic carbon materials. It can be produced by hydrocarbon decomposition over catalysts based on the iron group metals (Fe, Ni, Co) and their alloys (Ni–Cu, Fe–Co, Fe–Ni) [1–6]. CFC possesses a specific framework of fibers, which consist of graphene layers oriented in certain manner along the axis (angle α), forming "herring-bone" ($\alpha \sim 15$–45°), "platelet" ($\alpha \sim 90^\circ$) or multiwall carbon nanotubes (MWNTs) ($\alpha \sim 0^\circ$) structure in dependence of chemical nature of metal catalyst [1,7,8]. CFC is a predominantly mesoporous carbon with a large BET area varying from 100 to 300 m^2/g.

Among its potential practical applications are adsorbents for purification, magnetic and sensor materials. However, the use of these materials as catalyst supports seems the most promising due to its unique structural and textural properties. Such properties of CFC make it an attractive catalyst support that can display unusual behavior compared to classic supports. At present, numerous studies are focused at investigating CFC as supports for metal catalysts for liquid-phase selective hydrogenation reactions [9–11] and for gas-phase reactions [12–16]. In our previous works [13,17], we have used methane decomposition as a model reaction to study the catalytic properties of nickel supported on CFC. The best performance in this reaction has been observed with the supported Ni/CFC (Ni–Cu–Al_2O_3) catalyst prepared from nickel chloride precursor. Its superior properties are due to the formation of large (30–70 nm) Ni particles leading to the growth of new "secondary" carbon filaments. The yield of the secondary carbon has been shown to reach 240 g/g_{Ni} at 550 °C [13].

It has been known for a long time that textural properties of carbon materials can be modified by activation with water vapor, H_2 or CO_2 [18–23]. These treatments lead to the formation of a carbon material with the surface area and pore volume higher than that of the initial material. For this reason, the modification of textural properties of CFCs by their activation with H_2 or CO_2 opens up new areas for their application as catalyst supports.

---

[*] Corresponding author. Fax: +7 3832 343056.
E-mail address: t_reshetenko@mail.ru (T.V. Reshetenko).

0920-5861/$ – see front matter © 2005 Elsevier B.V. All rights reserved.
doi:10.1016/j.cattod.2005.02.011

Table 1
Production and characterization of the CFC supports

Support sample	Production of CFC				Textural and structural properties						
	Catalyst (wt.%)	T (°C)	G (g/g_{cat})	A_{BET} (m^2/g)	V_{meso} (cm^3/g)	V_{micro} (cm^3/g)	D_{BET} (nm)	V_{macro} (cm^3/g)	d_{002} (nm)	L_c (nm)	α (°)
CFC (Ni)	90Ni–Al_2O_3[a]	550	100	102.4	0.255	0.007	9.9	0.011	0.343	4.3	45
CFC (Ni–Cu)	65Ni–25Cu–Al_2O_3	625	291	260.7	0.405	0.014	6.2	0.116	0.341	5.2	90
CFC (Co)	75Co–Al_2O_3	500	45	116.4	0.585	0.001	20.1	1.024	0.344	3.3	15
CFC (Fe)	50Fe–Al_2O_3	625	26.5	151.5	0.501	0.007	13.2	2.050	0.343	8.7	0
CFC (Fe–Co)	50Fe–6Co–Al_2O_3	625	52.4	155.1	0.558	0.011	14.4	1.950	0.342	8.2	0
CFC (Fe–Ni)	62Fe–8Ni–Al_2O_3	625	142	151.0	0.663	0.011	17.5	2.720	0.343	4.1	0

[a] 90Ni–Al_2O_3 means that catalyst content is 90 wt.% metal Ni and 10 wt.% Al_2O_3.

The present work is devoted to study CFC as supports for Ni catalysts for low-temperature methane decomposition (525 °C) and the influence of the textural and structural properties of filamentous carbons on the efficiency of supported Ni/CFC catalysts.

2. Experimental

CFC supports were produced by methane decomposition over coprecipitated Ni–Al_2O_3 (CFC (Ni)), Ni–Cu–Al_2O_3 (CFC (Ni–Cu)), Co–Al_2O_3 (CFC (Co)), Fe–Al_2O_3 (CFC (Fe)), Fe–Co–Al_2O_3 (CFC (Fe–Co)) and Fe–Ni–Al_2O_3 (CFC (Fe–Ni)) catalysts with high metal loadings, as described elsewhere [4–6,24]. Table 1 presents the conditions of methane decomposition and structural parameters of CFC supports. CFC samples were treated with concentrated hydrochloric acid for 72 h to remove metal catalyst particles from the fibers. The treatment was followed by careful washing the CFC samples with water and drying at 110 °C.

Gasification of CFC (Ni) with H_2 ($T = 635$ °C) or with pure CO_2 ($T = 650$ °C) was carried out under atmospheric pressure with a gas flow rate equal to 2.25 l/h on 0.5 g of CFC. CFC burn-off was calculated using the next equation:

$$\text{Burn-off} = \frac{\Delta m_{\text{CFC}}}{m_{0,\text{CFC}}} \times 100\%.$$

Burn-off of the CFC (Ni) obtained after treatment was ca. 30–40%. The conditions of the gas treatment and textural CFC (Ni) properties are shown in Table 2.

The Ni/CFC catalysts were prepared by incipient wetness impregnation of carbon granules (0.5–1 mm) with aqueous $NiCl_2 \cdot 6H_2O$ solution [13]. Samples were kept in solution at ambient conditions for 12 h. Then, they were dried at ~100 °C for 2 h and calcined in N_2 at 350 °C for 2 h. The metal content determined by atomic adsorption spectroscopy was 10–15 wt.%. For catalytic tests, the samples were reduced in situ in H_2 flow (~5 l/h) at 350 °C for 3 h. Then, the temperature was elevated to 525 °C and undiluted methane was fed into the reactor. The activity measurements were carried out in a vibrating flow reactor at atmospheric pressure of methane and flow rate of 45 l/(g_{cat} h). Methane conversion (x, %) was determined by gas chromatography. Hydrogen and methane were detected and there are no any gas products. The amount of formed secondary CFC was determined by weighing samples before and after reaction. The reaction was continued until complete deactivation of the catalysts.

A URD-63 diffractometer with Cu Kα radiation was used for XRD studies. TEM pictures were acquired with a JEM-100CX microscope. Textural studies were performed on an ASAP-2400 (Micromeritics) automatic adsorption installation. Isotherms of N_2 adsorption at 77 K were used to calculate the surface area (A_{BET}) and total pore volume (V_{meso}). The values of V_{meso} at $P/P_0 = 0.98$ corresponded to pores with effective diameters up to 100 nm. In addition, pore size distributions were measured by mercury porosimetry (V_{macro}) using a PoreSiser-9300 (micromeritics).

3. Results and discussion

We used the following parameters to compare the carbon formation efficiency of prepared Ni/CFC catalysts in the methane decomposition reaction: methane conversion (x, %), carbon accumulation until complete deactivation of the catalysts (the so-called carbon capacity G, calculated as gram of carbon per gram of nickel, g/g_{Ni}) and lifetime of the catalysts (t, h).

Table 2
Conditions of CFC (Ni) activation and textural BET parameters

Sample	Conditions of activation			Textural properties				
	Gas	T (°C)	Burn-off (%)	A_{BET} (m^2/g)	V_{meso} (cm^3/g)	V_{micro} (cm^3/g)	D_{BET} (nm)	V_{macro} (cm^3/g)
CFC (Ni) + CO_2	CO_2	650	28.5	121.9	0.433	0.004	14.2	0.680
CFC (Ni) + H_2	H_2	635	40	125.6	0.494	0.003	17.5	0.760

Table 3
Catalytic properties of the 10–15 wt. % Ni/CFC in methane decomposition (Sample weight = 0.1 g, methane flow = 4.5 l/h, methane pressure = 1 atm)

Sample	Ni (wt.%)	T (°C)	t (h)	x (%)	G (g/g_{Ni})	Reference
Ni/CFC (Ni)	15	525	5	8	52	
Ni/(CFC (Ni) + CO_2)	10	525	11.5	12	229	
Ni/(CFC (Ni) + H_2)	10	525	12.75	9	238	
Ni/CFC (Ni–Cu)	15	525	16	10	224	
Ni/CFC (Co)	15	525	14.5	8.5	195.6	
Ni/CFC (Fe)	15	525	20	9	249.8	
Ni/CFC (Fe–Co)	15	525	12.5	8	193	
Ni/CFC (Fe–Ni)	15	525	20.5	8.5	268.5	
90Ni–Al_2O_3	90	525	30	11	199	
Ni/CFC (Ni)	15	550	2	8	33	[13]
Ni/CFC (Ni–Cu)[a]	15	550	17	8.5	245	[13]
Ni/carbon fiber (CH_4)	20	530	3.5	9	45	[16]
Ni/nanotubes	20	550	48	–	87.5	[15]
Decomposition of C_2H_6:H_2 = 30:100						

[a] CFC (Ni–Cu) was produced by methane decomposition at 575 °C on catalyst with composition 82Ni–8Cu–Al_2O_3.

The catalytic properties of the Ni/CFC are summarized in Table 3. The carbon capacity of Ni/CFC followed the order:

$$\begin{aligned}\mathrm{CFC(Fe{-}Ni)} &\geq \mathrm{CFC(Fe)} > (\mathrm{CFC(Ni)} + \mathrm{H_2}) \\ &= (\mathrm{CFC(Ni)} + \mathrm{CO_2}) = \mathrm{CFC(Ni{-}Cu)} > \mathrm{CFC(Co)} \\ &= \mathrm{CFC(Fe{-}Co)} \gg \mathrm{CFC(Ni)}.\end{aligned}$$

The results indicate that the carbon capacities of Ni/CFC, except for CFC (Ni), and coprecipitated 90Ni–Al_2O_3 are close. The maximum carbon yield reaches 268.5 g/g_{Ni} and is observed on Ni supported on the multiwall carbon nanotubes—CFC (Fe–Ni). Table 3 also presents G values for other carbon supported-Ni catalysts for CH_4 and C_2H_6 decomposition reactions reported in the literature. The obtained our results agree with the published data on carbon capacity of Ni/carbon catalysts for methane decomposition at close conditions.

The TEM micrograph of reduced Ni/CFC (Fe–Co) catalyst shows large metal particles (50–70 nm) and well-shaped Ni crystallites, which are localized between the carbon nanotubes (Fig. 1a). It should be noted that nickel crystallites are also 50–70 nm in size when supported on CFC of other types (Fig. 1b). Two types of the active component (Ni) localization sites on the filament support may be identified:

(1) basal graphene planes on the carbon nanotubes surface (CFC (Fe), CFC (Fe–Co), CFC (Fe–Ni)) and basal planes on the filament tips (CFC (Ni–Cu)); and
(2) steps and edges on the filament surface.

Based on literature data, one can suppose that the filament surface, which is determined by the filament microstructure, affects the formation of active catalytic particles. In principle, it is well known [25] that the surface enthalpies for graphite are 0.16 J/m^2 for basal planes and 6.3 J/m^2 for prismatic planes, and the linkage of surface edges should be thermodynamically favorable. Only a small part (5–10%) of the filament surface is represented by open edges of the graphene layers [7]. Thus, the surface of the carbon filaments of the effective supports seems to be represented predominantly by extended basal graphene planes. The interaction of metal particles with graphene basal planes

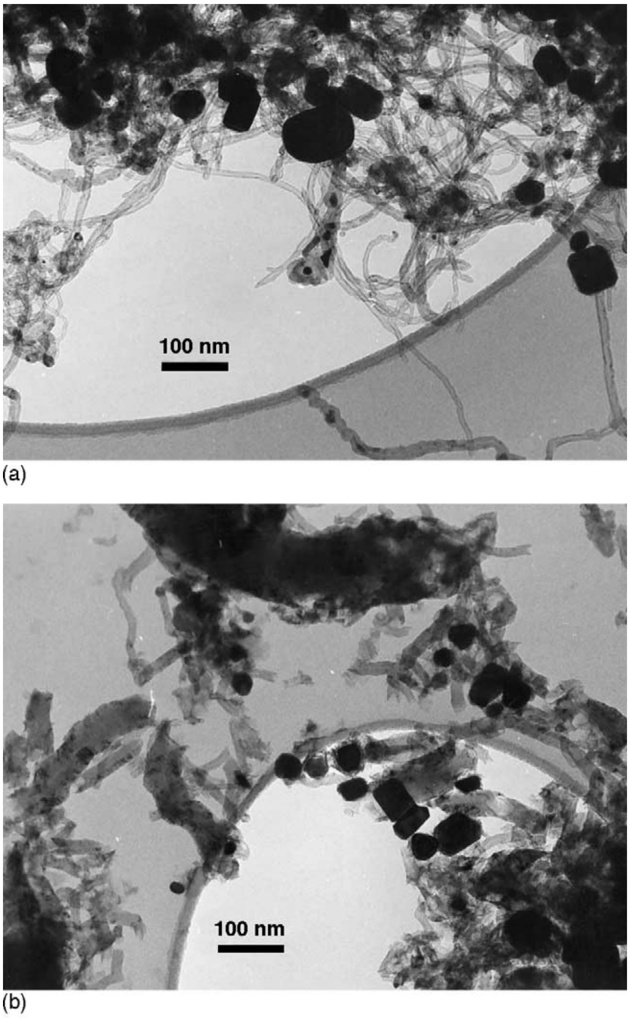

Fig. 1. TEM photographs of the reduced catalysts: (a) Ni/CFC (Fe–Co); and (b) Ni/(CFC (Ni) + H_2).

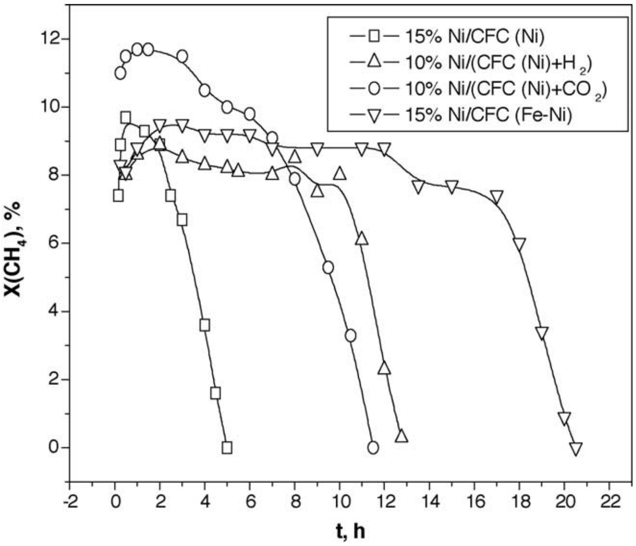

Fig. 2. Methane conversion as a function of time on the Ni/CFCs catalysts (525 °C, methane pressure = 1 atm, space velocity = 45 l/(g_{cat} h)).

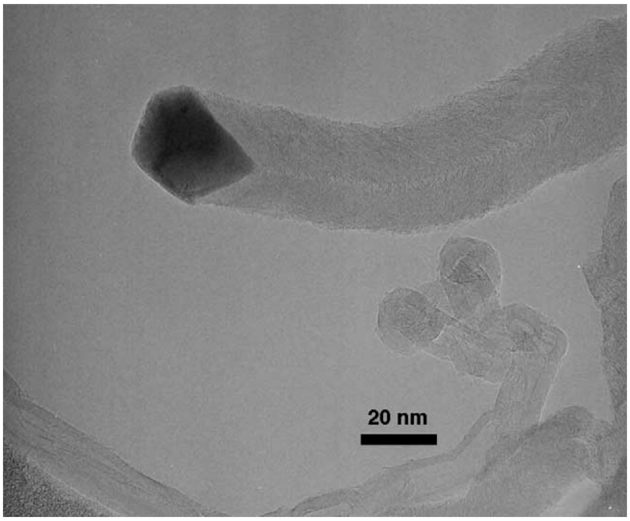

Fig. 3. TEM picture of the Ni/CFC (Fe–Co) after 40 min in methane decomposition at 525 °C.

occurs mainly through weak dispersive forces [10,11,14–16,26]. It results in a broad particle size distribution and, probably, in the formation of coarse metal particles. The Ni particles prepared from $NiCl_2$ precursor are known to be 20–35 nm in size both on oxide [27] and carbon [13,28] supports. Earlier it was suggested [13] that the interaction of nickel chloride precursor with CFC leads to generation of Ni particles, which are large enough to initialize the formation of filamentous carbon. Formation of the large nickel particles needs a considerable volume. Therefore, they are preferably localized in the pores formed by interlaced filaments and on the extended graphene basal planes. Hence, a requirement for textural properties of the support is that there must be a considerable volume of large pores.

The curves of methane conversion versus reaction time (Fig. 2) plotted for supported Ni/CFC catalysts are similar to those observed for coprecipitated Ni–Al_2O_3 systems with high metal loadings [4]. Both are characterized by weakly expressed induction periods. The induction period for coprecipitated Ni–Al_2O_3 catalyst relates to the formation of active centers (50 nm in size) due to agglomeration of initial 15–17 nm nickel particles oversaturated with carbon [4]. Therefore, the high activity of Ni/CFC can be accounted for by the size of Ni particles that is almost optimal for the filament growth. So, filamentous carbon are appropriate supports for synthesis of effective Ni/CFC catalysts for low-temperature methane decomposition due to formation of the active nickel particles (30–50 nm in size), which result from the preparation procedure of the catalysts and the influence of carbon supports.

Fig. 3 shows the TEM microphotograph of the Ni/CFC (Fe–Co) sample with secondary carbon produced by the reaction. One can see carbon nanotubes of the support and Ni particle located on the tip of the growing filament with "herring-bone" structure. The Ni particles in all studied samples are transformed into pear-shaped species identical to the ones usually observed in Ni–alumina catalysts [4]. Therefore, the shape of the metal particle and graphene layers arrangement in the new filament does not depend on the microstructure of the used carbon support. As the secondary CFC begins to grow upon methane decomposition, the catalytic particle escapes from the filament surface and, after that, exists independent from the support. Hence, there is no need in the strong metal-support interaction in this case. In general, the mechanism of the secondary carbon growth on Ni/CFC is likely to be the same as for coprecipitated Ni–Al_2O_3 [4,29]. The commonly accepted model of methane decomposition and carbon growth over nickel catalysts includes the stages of activation and decomposition of methane on (1 0 0) and (1 1 0) metal surface planes, carbon dissolution and diffusion through the particle, carbon segregation in the form of graphite-like phase on (1 1 1) nickel planes due to crystallographic matching of (1 1 1) nickel surface to (0 0 2) graphite planes [29].

The lowest activity to methane decomposition and carbon deposition is observed for Ni/CFC (Ni) (see Table 3). Notice that CFC (Ni) has a close packing of the filaments and a comparatively small volume of large pores (Table 1). It seems that all its pores are filled by carbon during the CFC growth, leading to diffusion limitations for the gas flow. Nevertheless Ni catalysts supported on the CFC (Ni) activated with H_2 or CO_2: (CFC (Ni) + H_2) and (CFC (Ni) + CO_2), demonstrate a high efficiency for accumulation of the secondary carbon. The rise of the carbon capacity may be accounted for by an increase of the meso- and macropore volume of the supports after the activation with H_2 or CO_2 (Table 2). The activation of CFC (Ni) in hydrogen and carbon dioxide apparently exerts a slight affect on the volume and surface area of pores less than 10 nm in size, the micropore volume V_{micro} being practically constant.

The observed transformations are mainly related to expansion of the volume and size of pores larger 10 nm in size (predominantly, those ranging from 15 to 30 nm in size). The whole set of textural transformations observed during the CFC gasification can be accounted for by the fact that only individual more disordered graphene packages (10–30 nm in size) undergo complete gasification to form mesopores of the corresponding size [30]. Whereas typical activation of ordinary carbon materials is based on successive increase of pore size and volume due to burning of graphene layeres: micropores first, then meso- and, eventually, macropores [20,31–33].

Based on the obtained results we would like to suggest that the following factors may be responsible for the formation of carbon-capacious Ni/CFC systems for low-temperature methane decomposition:

(1) textural properties of the support (the presence of pores larger than 100 nm in size, high porosity of the support);
(2) surface structure of the filament with exposed graphene basal planes provides weak metal support interaction that makes the system labile; and
(3) choice of the catalyst precursor ($NiCl_2$).

From this point of view the application of MWNTs (CFC (Fe), CFC (Fe–Co), CFC (Fe–Ni)) with high value of the pore volume allows for a new type of carbon materials to be synthesized—a CFC/CFC composite, in which every granule consists of two types of CFC with different filament structures: ‘‘herring-bone’’ and carbon nanotubes. The textural properties of these composites are close to the values characteristic for CFC (Ni) [8,17]. The BET surface area A_{BET} is 81–95 m^2/g, mesopore volume V_{meso} is 0.26–0.31 cm^3/g, mean pore size D_{BET} is 11–15 nm. The modification of the textural properties of CFC (Ni) by the activation with H_2 or CO_2 opens up interesting possibilities of its application as support in heterogeneous catalysis.

4. Conclusions

1. Ni/CFC catalysts were shown to have sufficient efficiency in secondary carbon formation in low-temperature methane decomposition (525 °C). The carbon capacity of Ni/CFCs followed the order: $\text{CFC (Fe–Ni)} \geq \text{CFC (Fe)} > (\text{CFC (Ni)} + H_2) = (\text{CFC (Ni)} + CO_2) = \text{CFC (Ni–Cu)} > \text{CFC (Co)} = \text{CFC (Fe–Co)} \gg \text{CFC (Ni)}$. The highest yield of secondary carbon was found to reach 268.5 g/g_{Ni} on Ni/CFC (Fe–Ni) catalyst.
2. The catalytic properties of Ni/CFCs may be explained by formation of active Ni particles (ca. 50 nm in size), which are optimal for filament growth. These Ni particles are preferably localized in the pores formed by interlaced filaments and the interaction of metal particles with graphene basal planes occurs mainly through weak dispersive forces.
3. The accumulation of carbon on Ni/CFC catalysts is also influenced by textural properties of the used supports. The CFC with high value of the meso- and macropore volume are likely to be more suitable for development of Ni/CFC catalysts for low-temperature methane decomposition. The modification of the textural properties of CFC (Ni) by the activation with H_2 or CO_2 opens up interesting possibilities of its application as support for Ni catalysts. We believe that CFC with textural and structural properties varied over wide range is a new promising carbon supports for metal catalysts.

Acknowledgements

We are grateful to Dr. V.A. Ushakov and Dr. S.V. Cherepanova for some XRD data. The researches described in this publication were supported by Award No. REC-008 from the U.S. Civilian Research and Development Foundation for the Independent States of the Former Soviet Union (CRDF) and by the Netherlands Organization for Scientific Research (NWO) in the year of 2001.

References

[1] N.M. Rodriguez, A. Chamber, R.T.K. Baker, Langmuir 11 (1995) 3862.
[2] V.V. Chesnokov, R.A. Buyanov, Russ. Chem. Rev. 69 (2000) 623.
[3] C.A. Bernardo, I. Alstrup, J.R. Rosrtup-Nielsen, J. Catal. 96 (1985) 517.
[4] L.B. Avdeeva, O.V. Goncharova, D.I. Kochubey, V.I. Zaikovskii, L.M. Plyasova, B.N. Novgorodov, Sh.K. Shaikhutdinov, Appl. Catal. A 141 (1996) 117.
[5] L.B. Avdeeva, D.I. Kochubey, Sh.K. Shaikhutdinov, Appl. Catal. A 177 (1999) 43.
[6] L.B. Avdeeva, T.V. Reshetenko, Z.R. Ismagilov, V.A. Likholobov, Appl. Catal. A 228 (2002) 53.
[7] V.B. Fenelonov, A.Yu. Derevyankin, L.G. Okkel, L.B. Avdeeva, V.I. Zaikovskii, E.M. Moroz, A.N. Salanov, N.A. Rudina, V.A. Likholobov, Sh.K. Shaikhutdinov, Carbon 35 (1997) 1129.
[8] T.V. Reshetenko, L.B. Avdeeva, Z.R. Ismagilov, V.V. Pushkarev, S.V. Cherepanova, L.A. Chuvilin, V.A. Likholobov, Carbon 41 (2003) 1605.
[9] J.M. Planeix, N. Coustel, B. Coq, V. Brotons, P.S. Kumbhar, R. Dutartre, P. Geneste, P. Bernier, P.M. Ajayan, J. Am. Chem. Soc. 116 (1994) 7935.
[10] F. Salmon, C. Park, R.T.K. Baker, Catal. Today 53 (1999) 385.
[11] C. Pham-Huu, N. Keller, G. Ehret, L.J. Charboniere, R. Ziessel, M.J. Ledoux, J. Mol. Catal. A 170 (2001) 155.
[12] N.M. Rodriguez, M.-S. Kim, R.T.K. Baker, J. Phys. Chem. 98 (1994) 13108.
[13] Sh.K. Shaikhutdinov, L.B. Avdeeva, B.N. Novgorodov, V.I. Zaikoskii, D.I. Kochubey, Catal. Lett. 47 (1997) 35.
[14] P.E. Anderson, N.M. Rodriguez, Chem. Mater. 12 (2000) 823.
[15] C. Pham-Huu, N. Keller, V.V. Roddatis, G. Mestl, R. Schlögl, M.J. Ledoux, Phys. Chem. Chem. Phys. 4 (2002) 514.
[16] K. Otsuka, H. Ogihara, S. Takenaka, Carbon 41 (2003) 223.
[17] T.V. Reshetenko, L.B. Avdeeva, Z.R. Ismagilov, A.L. Chuvilin, Carbon 42 (2004) 143.
[18] P.L. Walker Jr., J.F. Rusinko Jr., L.G. Austin, Adv. Catal. 11 (1959) 133.
[19] T. Wigmans, Carbon 27 (1989) 13.

[20] V.B. Fenelonov, Porous carbon, Novosibirsk (1995) 206.
[21] M. Molina-Sabio, M.T. Gonzalez, F. Rodriguez-Reinoso, A. Sepulveda-Escribano, Carbon 34 (1996) 505.
[22] A. Tomita, Catal. Surv. Jpn. 5 (2001) 17.
[23] A. Ahmadpour, D.D. Do, Carbon 34 (1996) 471.
[24] T.V. Reshetenko, L.B. Avdeeva, Z.R. Ismagilov, A.L. Chuvilin, V.A. Ushakov, Appl. Catal. A 247 (2003) 247.
[25] J. Abrahamson, Carbon 11 (1973) 337.
[26] J. Ma, C. Park, N.M. Rodriguez, R.T.K. Baker, J. Phys. Chem. B 105 (2001) 11994.
[27] C. Hoang-Van, Y. Kachaya, S.J. Teichner, Y. Arnaud, J.A. Dalmon, Appl. Catal. A 46 (1989) 281.
[28] M. Domingo-Garsia, L. Vicente-Gutierrez, C. Moreno-Castilla, React. Kinet. Catal. Lett. 43 (1991) 93.
[29] R.T. Yang, J.P. Chen, J. Catal. 115 (1989) 52.
[30] L.B. Avdeeva, T.V. Reshetenko, V.B. Fenelonov, A.L. Chuvilin, Z.R. Ismagilov, Carbon 42 (2004) 2501.
[31] H.F. Stoeckli, L. Ballerini, S. de Bernardi, Carbon 27 (1989) 501.
[32] P.J.M. Carrot, J.J. Freeman, Carbon 29 (1991) 499.
[33] I.M.K. Ismail, Carbon 28 (1990) 401.